



Inorganic and organometallic cobaloximes with dioxime containing Se side chain: Synthesis, characterization and comparison with related B₁₂ model compounds

Kamlesh Kumar*, Bhagwan D. Gupta[†]

Department of Chemistry, Indian Institute of Technology, Kanpur 208 016, India

ARTICLE INFO

Article history:

Received 29 April 2011

Received in revised form

9 July 2011

Accepted 11 July 2011

Keywords:

Bis(phenylselanyl)glyoxime

Cobaloxime

Reactivity

X-ray structure

ABSTRACT

New series of cobaloximes, RCo(dSePhgH)₂Py (R = Cl, Me, Et, *n*-Pr, *n*-Bu, Bn, 4-ClC₆H₄CH₂) have been synthesized and characterized by NMR and elemental analysis. Molecular oxygen insertion in the benzyl complexes under photochemical conditions has been carried out and a comparison of its reaction rate with other similar cobaloximes gives the order dmestgH > dSePhgH > dpgh > dSPhgH ≥ dmgH > gH. The molecular structures of ClCo(dSePhgH)₂Py, MeCo(dSePhgH)₂Py, BnCo(dSePhgH)₂Py, 4-ClC₆H₄CH₂Co(dSePhgH)₂Py and a dioxy complex Bn(O₂)Co(dSePhgH)₂Py have been determined by X-ray crystallography. The SePh groups in these complexes adopt either up-down, up-down or down-down, down-down conformations in the solid state depending upon the steric bulk and steric interactions with the axial ligand and also their orientation affects the NMR chemical shifts.

© 2011 Elsevier B.V. All rights reserved.

1. Introduction

In the past four decades a significant effort has been devoted to the synthesis and characterization of simple cobalt complexes containing a stable Co–C σ bond [1–3] and systematic investigations have been made to understand the strength of the Co–C bond as a function of steric and electronic factors with a wide range of axial ligands in cobaloximes [3]. The studies have helped to understand the chemistry and biochemistry of B₁₂ coenzymes [4–6]. The influence of equatorial ligands (*cis* influence) in the Schiff base compounds like Co(saloph)R (saloph = dianion of disalicylidene-*o*-phenylenediamine) [7,8], LCo(acacen)R [acacen = dianion of ethylenebis(acetylacetonate imine)] [1], LCo(salen)R [salen = dianion of *N,N'*-ethylenebis(salicylideneamine)] [9] and Costa's model [10,11] such as [LCo{(DO)(DOH)pn}R]X [(DO)(DOH)pn, *N*²,*N*²-propanediylbis(2,3-butanedione-2-imine-3-oxime)] has also been reported.

The most extensively studied cobaloximes have dmgH as equatorial ligand and studies with other dioximes such as gH [12–15], chgH [16–18], dpgh [19–21], dmestgH [22,23], and dSPhgH [24] are few. The studies strongly suggest that the Co–C bond stability/reactivity is significantly affected by the equatorial dioximes (*cis* effect and *cis* influence). Hence, there has been a sustained interest to synthesize cobaloximes in which the

electronic and steric bulk properties of the dioxime are altered. Our recent work on cobaloximes with dSPhgH [24] has shown that the S side chain in the dioxime also plays an important role in the Co–C bond stability/reactivity. With these objectives in mind we have synthesized and characterized cobaloximes (1–7) with dioximes having SePh side chain i.e. bis(phenylselanyl)glyoxime (Scheme 1). All complexes are new and are reported for the first time. The molecular structures of 1, 2, 6 and 7 have been determined by single-crystal X-ray diffraction. The molecular oxygen insertion and their rate in the benzyl complexes 6 and 7 have also been carried out. The structural features of the dioxy complex (8) are described.

2. Experimental section

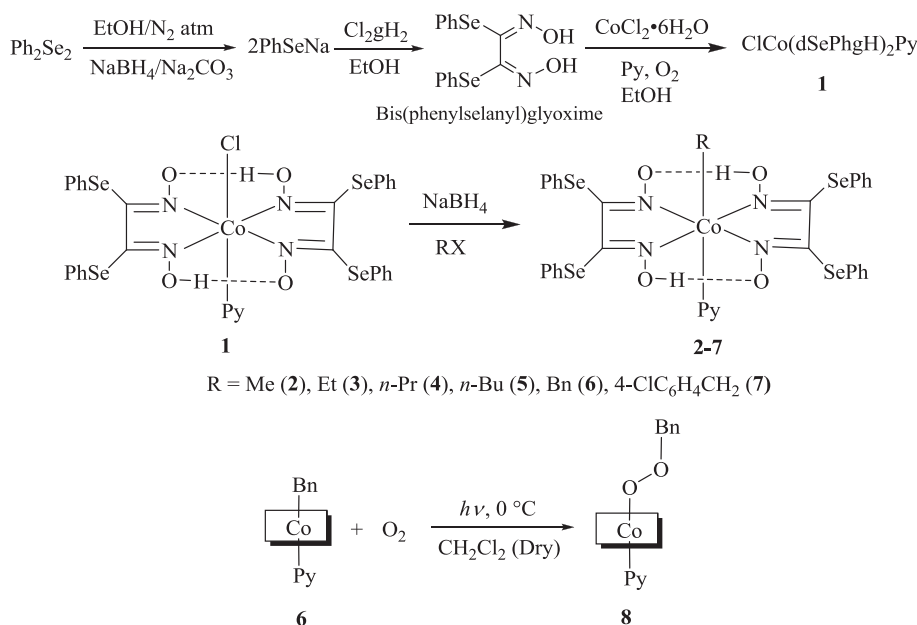
2.1. Materials and physical measurements

CoCl₂·6H₂O (SD Fine, India), diphenyl diselenide, iodomethane, iodoethane, 1-bromobutane, 1-bromopropane, benzyl chloride, and 4-chlorobenzyl chloride (all Sigma–Aldrich, USA) were used as received without further purifications. Dichloroglyoxime was prepared and purified by reported literature procedure [24]. Silica gel (100–200 mesh) and distilled solvents were used in all reactions and in chromatographic separations. A Julabo UC-20 low-temperature refrigerated circulator was used to maintain the desired temperature. ¹H and ¹³C spectra were recorded on a JEOL ECX-500 FT NMR Spectrometer (500 MHz for ¹H and 125 MHz for ¹³C) in CDCl₃ with TMS as internal standard. Elemental analyses for C, H and N were performed on CE-440 Elemental Analyzer. The

* Corresponding author. Tel.: +91 512 2597730; fax: +91 512 2597436.

E-mail address: kamlesh@iitk.ac.in (K. Kumar).

[†] Prof. Bhagwan D. Gupta deceased on 31 March 2011.



Scheme 1. Synthesis of cobaloximes [1–7] and oxygen insertion reaction in complex 6.

kinetic studies were performed on an Ocean Optics USB4000 (BASI, USA) UV–vis spectrometer in dry CH₂Cl₂. Cyclic voltammetry measurements were carried out using a BAS Epsilon electrochemical work station with a platinum working electrode, a Ag/AgCl reference electrode (3 M NaCl) and a platinum-wire counter electrode. All measurements were performed in 0.1 M ⁿBu₄NPF₆ in CH₂Cl₂ (dry) at a concentration of 1 mM of each complex.

2.2. X-ray crystal structure determination and refinements

X-ray crystallographic data were collected using graphite-monochromated Mo-K α radiation ($\lambda = 0.71073 \text{ \AA}$) on “Bruker SMART APEX CCD diffractometer” at 100 K. The linear absorption coefficients, scattering factors for the atoms and the anomalous dispersion corrections were taken from the *International Tables for X-ray Crystallography* [25]. The program SMART [26] was used for collecting frames of data, indexing reflections, and determining lattice parameters. The data integration and reduction were processed with SAINT software [26]. An empirical absorption correction was applied to the collected reflections with SADABS [27] using XPREP [28]. All the structures were solved by the direct method using the program SHELXS-97 [29] and were refined on F^2 by the full-matrix least-squares technique using the SHELXL-97 [29] program package. All non-hydrogen atoms were refined with anisotropic displacement parameters in all the structures. The hydrogen atom positions or thermal parameters were not refined but were included in the structure factor calculations. The ‘SQUEEZE’ option in PLATON was used to remove disordered solvent molecule from the overall intensity data in complex 8. The pertinent crystal data and refinement parameters for compounds 1, 2, 6, 7 and 8 are compiled in Table 1.

2.3. Syntheses

2.3.1. Synthesis of bis(phenylselanyl)glyoxime (dSePhgH₂)

A degassed solution of NaBH₄ (0.076 g, 2 mmol) in 1 mL water was added drop wise to the solution of diphenyl diselenide (0.321 g, 1 mmol) in 20 mL dry ethanol under nitrogen atmosphere. On completion of the addition, a degassed saturated solution of Na₂CO₃ was added drop wise until the reaction mixture became colorless. A

solution of dichloroglyoxime (0.157 g, 1 mmol) in 10 mL dry ethanol was added to the colorless solution with constant stirring and the reaction mixture was stirred further for 12 h. Filtration was done to remove any precipitate and the filtrate was kept aside for slow evaporation of solvent. The solid crystalline compound so obtained was washed with CH₂Cl₂ and dried under vacuum. Yield: 0.318 g (~79%). The same yield was obtained when the reaction was scaled up five times. ¹H NMR (500 MHz, CDCl₃+DMSO-*d*₆, δ ppm): 7.53 (4H, d, $J = 6.8 \text{ Hz}$), 7.39–7.28 (6H, m), N–O \cdots H = 11.84 (s). ¹³C NMR (125 MHz, CDCl₃+DMSO-*d*₆, δ ppm): 143.78, 137.06, 128.94, 128.79, 125.49. Anal. Calcd for C₁₄H₁₂N₂O₂Se₂: C, 42.23; H, 3.04; N, 7.04. Found: C, 42.39; H, 2.99; N, 7.10.

2.3.2. Synthesis of ClCo(dSePhgH₂)₂Py (1)

In a typical reaction, a solution of CoCl₂·6H₂O (0.100 g, 0.420 mmol) in 10 mL ethanol was added to a stirred solution of bis(phenylselanyl)glyoxime (0.398 g, 0.840 mmol) in 15 mL ethanol followed by the addition of pyridine 0.160 mL (2.0 mmol). The stirring was continued further for 30 min and air was passed through the solution for 2 h with occasional swirling. The solid crude product was filtered, washed with water and dried over P₂O₅ and purified on a silica gel column using CH₂Cl₂ as eluent. Yield: 0.220 g (~54%). ¹H NMR (500 MHz, CDCl₃, δ ppm): Py α = 7.85 (2H, d, $J = 5.6 \text{ Hz}$), Py γ = 7.76 (1H, t, $J = 7.7 \text{ Hz}$), 7.26–7.21 (12H, m), 7.15–7.08 (10H, m), 18.04 (2H, s, O–H \cdots O). ¹³C NMR (125 MHz, CDCl₃, δ ppm): 150.93 (Py α), 143.26 (C=N, C_q), 138.95 (Py γ), 132.72, 129.38, 128.42, 128.13, 125.99. Anal. Calcd for C₃₃H₂₇ClCoN₅O₄Se₄: C, 40.95; H, 2.81; N, 7.24. Found: C, 41.06; H, 2.77; N, 7.21.

2.3.3. Synthesis of RCo(dSePhgH₂)₂Py (2–7): General procedure

A few drops of aqueous NaOH were added to the suspension of ClCo(dSePhgH₂)₂Py (0.100 g, 0.103 mmol) in 25 mL CH₃OH and N₂ gas was bubbled through the solution with stirring for 20 min. Addition of pyridine (0.016 g, 0.206 mmol) followed by aqueous NaBH₄ (0.020 g, 0.529 mmol) at 0 °C turned the solution blue.¹ The solution turned reddish-orange on addition of alkyl/benzyl halide

¹ Pyridine must be added prior to the addition of NaBH₄, otherwise the precipitation occurs.

Table 1
Crystal data and structure refinement details for **1**, **2**, **6**, **7** and **8**.

parameters	1	2	6	7	8
Empirical formula	C ₃₃ H ₂₇ ClCoN ₅ O ₄ Se ₄	C ₃₄ H ₃₀ CoN ₅ O ₄ Se ₄	C ₄₀ H ₃₄ CoN ₅ O ₄ Se ₄	C ₄₀ H ₃₃ ClCoN ₅ O ₄ Se ₄	C ₄₀ H ₃₄ CoN ₅ O ₆ Se ₄
Formula weight	967.82	947.40	1023.49	1057.93	1055.49
Temp (K)	100(2)	100(2)	100(2)	100(2)	100(2)
Crystal system	Orthorhombic	Orthorhombic	Monoclinic	Monoclinic	Monoclinic
Space group	<i>Pbcm</i>	<i>Pbcm</i>	<i>P2₁/c</i>	<i>P2₁/c</i>	<i>P2₁/c</i>
Unit cell dimension					
<i>a</i> (Å)	10.824(4)	10.907(3)	18.664(5)	18.316(5)	11.9113(17)
<i>b</i> (Å)	13.179(5)	13.048(4)	12.647(5)	13.942(4)	22.160(3)
<i>c</i> (Å)	24.050(8)	24.257(7)	17.696(5)	16.629(5)	15.508(2)
α (deg)	90.00	90.00	90.000(5)	90.00	90.00
β (deg)	90.00	90.00	113.024(5)	113.927(5)	104.356(3)
γ (deg)	90.00	90.00	90.000(5)	90.00	90.00
<i>V</i> (Å ³)	3431(2)	3452.2(18)	3844(2)	3881.7(18)	3965.7(10)
<i>Z</i>	4	4	4	4	4
ρ (calc), g/cm ³	1.874	1.823	1.768	1.810	1.768
μ (Mo-K α), mm ⁻¹	4.868	4.761	4.283	4.311	4.158
<i>F</i> (000)	1888	1856	2016	2080	2080
Crystal size (mm ³)	0.43 × 0.32 × 0.18	0.37 × 0.23 × 0.17	0.43 × 0.31 × 0.22	0.32 × 0.22 × 0.18	0.42 × 0.31 × 0.19
Index ranges	−13 ≤ <i>h</i> ≤ 13 −16 ≤ <i>k</i> ≤ 16 −15 ≤ <i>l</i> ≤ 29	−13 ≤ <i>h</i> ≤ 10 −15 ≤ <i>k</i> ≤ 15 −28 ≤ <i>l</i> ≤ 29	−22 ≤ <i>h</i> ≤ 20 −11 ≤ <i>k</i> ≤ 15 −21 ≤ <i>l</i> ≤ 20	−24 ≤ <i>h</i> ≤ 17 −17 ≤ <i>k</i> ≤ 18 −19 ≤ <i>l</i> ≤ 22	−14 ≤ <i>h</i> ≤ 14 −26 ≤ <i>k</i> ≤ 26 −18 ≤ <i>l</i> ≤ 12
No. of rflns collected	18 222	17 422	20 199	24 896	21 027
No. of indep rflns	3447	3278	7108	9500	7331
GOOF on <i>F</i> ²	1.058	1.048	1.005	1.059	1.009
Final <i>R</i> indices (<i>I</i> > 2 σ (<i>I</i>))	<i>R</i> 1 = 0.0492 <i>wR</i> 2 = 0.1118	<i>R</i> 1 = 0.0404 <i>wR</i> 2 = 0.0900	<i>R</i> 1 = 0.0462 <i>wR</i> 2 = 0.0956	<i>R</i> 1 = 0.0598 <i>wR</i> 2 = 0.1300	<i>R</i> 1 = 0.0486 <i>wR</i> 2 = 0.1115
<i>R</i> indices (all data)	<i>R</i> 1 = 0.0747 <i>wR</i> 2 = 0.1498	<i>R</i> 1 = 0.0620 <i>wR</i> 2 = 0.1010	<i>R</i> 1 = 0.0763 <i>wR</i> 2 = 0.1092	<i>R</i> 1 = 0.1139 <i>wR</i> 2 = 0.1901	<i>R</i> 1 = 0.0784 <i>wR</i> 2 = 0.1290
Data/restraints/param	3447/3/235	3278/8/236	7108/0/473	9500/1/504	7331/22/513

(0.206 mmol). The stirring was continued at 0 °C for 1 h. The reaction mixture was slowly brought to room temperature and was poured in ice cold water (20 mL). The resulting reddish-orange precipitate was filtered, washed with ice-cold water and dried. The crude product was purified by column chromatography using CH₂Cl₂ as eluent.

2.3.3.1. MeCo(dSePhgH)₂Py (2). Yield: 0.055 g (~56%). ¹H NMR (500 MHz, CDCl₃, δ ppm): Py α = 8.22 (2H, d, *J* = 5.2 Hz), Py γ = 7.83 (1H, t, *J* = 7.1 Hz), 7.23–7.07 (22H, m), 1.06 (3H, s, CoCH₃), 18.28 (2H, s, O–H...O). ¹³C NMR (125 MHz, CDCl₃, δ ppm): 149.83 (Py α), 139.85 (C=N, C_q), 137.74 (Py γ), 132.69, 129.12, 128.89, 127.77, 125.54, 12.26 (CH₃). Anal. Calcd for C₃₄H₃₀CoN₅O₄Se₄: C, 43.10; H, 3.19; N, 7.39. Found: C, 42.97; H, 3.17; N, 7.44.

2.3.3.2. EtCo(dSePhgH)₂Py (3). Yield: 0.053 g (~53%). ¹H NMR (500 MHz, CDCl₃, δ ppm): Py α = 8.19 (2H, d, *J* = 5.2 Hz), Py γ = 7.83 (1H, t, *J* = 7.1 Hz), 7.24–7.05 (22H, m), 1.97 (2H, q, *J* = 7.8 Hz, CoCH₂), 0.35 (3H, t, *J* = 7.8 Hz), 18.20 (2H, s, O–H...O). ¹³C NMR (125 MHz, CDCl₃, δ ppm): 149.87 (Py α), 139.57 (C=N, C_q), 137.57 (Py γ), 132.95, 129.04, 128.84, 127.78, 125.48, 29.09 (CH₂), 16.19 (CH₃). Anal. Calcd for C₃₅H₃₂CoN₅O₄Se₄: C, 43.72; H, 3.35; N, 7.28. Found: C, 43.89; H, 3.39; N, 7.34.

2.3.3.3. n-PrCo(dSePhgH)₂Py (4). Yield: 0.041 g (~41%). ¹H NMR (500 MHz, CDCl₃, δ ppm): Py α = 8.21 (2H, d, *J* = 4.6 Hz), Py γ = 7.82 (1H, t, *J* = 7.5 Hz), 7.23–7.05 (22H, m), 1.79 (2H, t, *J* = 8.7 Hz, CoCH₂), 0.94–0.86 (2H, m), 0.73 (3H, t, *J* = 7.1 Hz), 18.20 (2H, s, O–H...O). ¹³C NMR (125 MHz, CDCl₃, δ ppm): 149.97 (Py α), 139.82 (C=N, C_q), 137.71 (Py γ), 133.12, 129.17, 128.93, 127.93, 125.62, 37.65 (CoCH₂), 24.12 (CH₂), 14.49 (CH₃). Anal. Calcd for C₃₆H₃₄CoN₅O₄Se₄: C, 44.33; H, 3.51; N, 7.18. Found: C, 44.18; H, 3.48; N, 7.22.

2.3.3.4. n-BuCo(dSePhgH)₂Py (5). Yield: 0.046 g (~45%). ¹H NMR (500 MHz, CDCl₃, δ ppm): Py α = 8.22 (2H, d, *J* = 5.2 Hz), Py γ = 7.81 (1H, t, *J* = 7.7 Hz), 7.23–7.05 (22H, m), 1.83 (2H, t, *J* = 8.8 Hz, CoCH₂),

1.19–1.15 (2H, m), 0.93–0.88 (2H, m), 0.79 (3H, t, *J* = 7.4 Hz), 18.20 (2H, s, O–H...O). ¹³C NMR (125 MHz, CDCl₃, δ ppm): 149.95 (Py α), 139.77 (C=N, C_q), 137.71 (Py γ), 133.12, 129.18, 128.97, 127.92, 125.63, 35.15 (CoCH₂), 32.94 (CH₂), 23.67 (CH₂), 13.89 (CH₃). Anal. Calcd for C₃₇H₃₆CoN₅O₄Se₄: C, 44.91; H, 3.67; N, 7.08. Found: C, 45.07; H, 3.62; N, 7.04.

2.3.3.5. BnCo(dSePhgH)₂Py (6). Yield: 0.060 g (~57%). ¹H NMR (500 MHz, CDCl₃, δ ppm): Py α = 8.09 (2H, d, *J* = 4.6 Hz), Py γ = 7.80 (1H, t, *J* = 7.5 Hz), 7.17–7.12 (6H, m), 7.05–6.99 (19H, m), 6.94 (2H, d, *J* = 7.5 Hz), 3.08 (2H, s, CoCH₂), 18.25 (2H, s, O–H...O). ¹³C NMR (125 MHz, CDCl₃, δ ppm): 150.08 (Py α), 140.02 (C=N, C_q), 137.59 (Py γ), 132.84, 129.02, 128.94, 128.07, 127.64, 125.38, 125.32, 33.92 (CH₂). Anal. Calcd for C₄₀H₃₄CoN₅O₄Se₄: C, 46.94; H, 3.35; N, 6.84. Found: C, 47.03; H, 3.33; N, 6.81.

2.3.3.6. 4-ClC₆H₄CH₂Co(dSePhgH)₂Py (7). Yield: 0.069 g (~63%). ¹H NMR (500 MHz, CDCl₃, δ ppm): Py α = 8.08 (2H, d, *J* = 5.2 Hz), Py γ = 7.81 (1H, t, *J* = 7.8 Hz), 7.20–7.02 (22H, m), 6.95 (2H, d, *J* = 8.4 Hz), 6.79 (2H, d, *J* = 8.4 Hz), 2.96 (2H, s, CoCH₂), 18.14 (2H, s, O–H...O). ¹³C NMR (125 MHz, CDCl₃, δ ppm): 150.06 (Py α), 140.11 (C=N, C_q), 137.69 (Py γ), 133.00, 132.78, 129.96, 129.09, 128.98, 128.87, 128.12, 127.78, 125.44. Anal. Calcd for C₄₀H₃₃CoN₅O₄Se₄Cl: C, 45.41; H, 3.14; N, 6.62. Found: C, 45.30; H, 3.17; N, 6.65.

2.3.4. Molecular oxygen insertion in **6**: synthesis of BnO₂Co(dSePhgH)₂Py (**8**)

A solution of **6** (0.050 g) in 15 mL dry CH₂Cl₂ was irradiated at 0 °C with a 200 W tungsten lamp kept at a distance of approximately 10 cm and pure oxygen gas was bubbled into this solution for 1 h. The evaporation of solvent under reduced pressure afforded the crude product which was further purified on the silica gel column using 5% EtOAc/CH₂Cl₂ mixture solvent as eluent. Yield: 0.041 g (~79%). ¹H NMR (500 MHz, CDCl₃, δ ppm): Py α = 7.98 (2H, d, *J* = 5.2 Hz), Py γ = 7.75 (1H, t, *J* = 7.8 Hz), 7.32–7.27 (5H, m), 7.16–7.10 (14H, m), 6.99 (8H, t, *J* = 7.8 Hz), 4.30 (2H, s, O₂CH₂), 18.29 (2H, s,

O–H···O). ^{13}C NMR (125 MHz, CDCl_3 , δ ppm): 150.90 (Py α), 142.29 (C=N, C $_q$), 138.35 (Py γ), 136.81, 132.88, 132.76, 129.47, 129.14, 128.17, 127.91, 125.69, 125.59, 78.47 (OCH $_2$). Anal. Calcd for $\text{C}_{40}\text{H}_{34}\text{Co-N}_5\text{O}_6\text{Se}_4$: C, 45.52; H, 3.25; N, 6.64. Found: C, 45.69; H, 3.28; N, 6.75.

2.4. Kinetic study

The kinetics of oxygen insertion in the Co–C bond of complexes **6** and **7** under photochemical conditions were monitored spectrophotometrically at 0 °C under pseudo-first-order conditions. Oxygen was bubbled through the solution and hence used in large excess. The progress of the reaction was monitored following the changes (decreases) in absorbance (the absorbance due to the Co–C CT band around 460 nm) at regular intervals. Ocean Optics software in the UV–vis machine allows continuous scan for the change in absorbance at a particular wavelength with time. The k_{obs} rate constants were obtained from the slope of the linear plots of $\ln(A_t - A_\infty)$, versus time, where A_t is the absorbance at time t and A_∞ is the final absorbance. Kinetic data were analyzed with ORIGIN 8.

3. Results and discussion

3.1. Synthesis

Bis(phenylselanyl)glyoxime (dSePhgH $_2$) was prepared from sodium benzeneselenolate and dichloroglyoxime in ethanol solvent (Scheme 1). Aerial oxidation of the stoichiometric mixture of $\text{CoCl}_2 \cdot 6\text{H}_2\text{O}$, dSePhgH $_2$ and pyridine in ethanol formed $\text{ClCo}(\text{dSePhgH})_2\text{Py}$, similar to the known chlorocobaloximes with other dioximes. The oxidative alkylation of $\text{Co}^{\text{I}}(\text{dSePhgH})_2\text{Py}$ with alkyl/benzyl halide in CH_3OH under an inert atmosphere formed organocobaloximes **2–7**. The preparation, unlike the other reported organocobaloximes, required the addition of pyridine before the addition of NaBH_4 otherwise the precipitation occurred which led to very low yield of the product. Molecular oxygen insertion in **6** under photolytic conditions at 0 °C formed the dioxy compound (**8**) within 1 h in good yield.

3.2. Spectroscopy

All complexes (**1–8**) and dSePhgH $_2$ have primarily been characterized by ^1H and ^{13}C NMR spectroscopy and the spectral data are summarized in Experimental Section. The dioxime dSePhgH $_2$ is partially soluble in CDCl_3 and a drop of $\text{DMSO}-d_6$ is necessary to dissolve it. The ^1H NMR spectra of these complexes are easily assigned on the basis of the chemical shifts. The signals are assigned according to their relative intensities and are consistent with the related alkyl and benzyl cobaloximes with gH, dmHgH, dpHgH and dSPHgH. The ^1H Py β resonance is obscured in all the complexes.

The *cis* and *trans* influence study includes the investigation of all possible steric and electronic effects of the dioxime on the axial ligands and vice versa. The NMR studies of cobaloximes have shown that Py α and the α -carbon bonded to cobalt are most affected by the variation in equatorial dioxime [22,24]. Py α protons in **2–7** show considerable upfield shift as compared to the corresponding gH, dmHgH, chgH, dpHgH and dmestgH complexes and this upfield shift is similar to the dSPHgH complexes. Overall, ($\Delta\delta^1\text{Hpy}\alpha$) follows the upfield shift order dmestgH < dpHgH < gH \approx dmHgH \approx chgH < dSPHgH \approx dSePhgH (Table S1). This high upfield shift occurs by the shielding of Py α protons by the magnetic anisotropy of the phenyl ring of SePh groups.

The effect of *cis* influence on the chemical shift of Co–CH $_2$ protons in complexes **2–7** is similar to dSPHgH and follows the order dmHgH < gH < dSePhgH \approx dSPHgH < dpHgH < dmestgH (Table S2).

The extent of electron density on the $\text{Co}(\text{dioxime})_2$ chelate ring for different dioximes (keeping R/X and Py constant) can be

understood by comparing the $\Delta\delta(^{13}\text{C}_{\text{C=N}})$ [30] values of the dioxime in $\text{R}/\text{XCo}(\text{dioxime})_2\text{Py}$. The upfield shift $\Delta\delta(^{13}\text{C}_{\text{C=N}})$ is smaller in **2–7** as compared to the corresponding gH, dmHgH and dpHgH complexes but is larger than the dSPHgH and dmestgH analogues (Table S3) and follows the order gH > dmHgH > dpHgH > dSePhgH > chgH > dSPHgH > dmestgH. This means that the charge density on $\text{Co}(\text{dioxime})_2$ in **2–7** is higher than the dSPHgH and dmestgH complexes.

The chemical shifts of RCH $_2$ and Py α are further affected in the dioxy complex **8**. CH $_2$ –O $_2$ is shifted downfield by 1.22 ppm in ^1H NMR and 44.55 ppm in ^{13}C NMR as compared to **6**. ^1H Py α resonance appears upfield (0.11 ppm) and $^{13}\text{C}_{\text{C=N}}$ signal appears downfield by 2.27 ppm as compared to **6**. The data points to the higher cobalt anisotropy in the dioxy complex **8** than **6**.

3.3. X-ray crystallographic studies. Description of the molecular structures of **1**, **2**, **6** and **7**

Single-crystals suitable for X-ray crystallographic analyses were obtained by slow evaporation of solvent from the solution of complexes **1**, **2**, **6** and **7** ($\text{CH}_2\text{Cl}_2/\text{CH}_3\text{OH}$). Molecular structures along with selected numbering scheme are shown in Figs. 1–4 and selected bond lengths, bond angles and structural parameters are given in Table 2. It can be seen from Figs. 1–4 that all complexes have distorted octahedral geometry around the central cobalt atom with four nitrogen atoms of the dioxime (dSePhgH) in the equatorial plane and, pyridine and Cl (Me or Bn) are axially coordinated. Complexes **1** and **2** have a symmetry plane, and the molecular building blocks are formed by a symmetric operation on one asymmetric unit. The benzyl group in complexes **6** and **7** is located over the dioxime wing and shows some interaction with the dioxime ring current similar to the reported benzyl cobaloximes [31,32].

The Co–Cl or Co–C bond distances [2.224(2), 1.992(5) Å] and Co–N $_{\text{py}}$ bond distances [1.971(6), 2.064(5) Å] in **1** and **2** are almost identical with the reported values in the corresponding Cl/MeCo(dioxime) $_2$ Py complexes (Table S4). The Co–C [2.077(5), 2.073(6) Å] and Co–N $_{\text{py}}$ bond distances [2.070(4), 2.061(5) Å] in the benzyl complexes **6** and **7** do not differ significantly and also they are comparable with the reported values in $\text{BnCo}(\text{dSPHgH})_2\text{Py}$ (Table S5). As expected, the data in Table 2 show that the Co–C

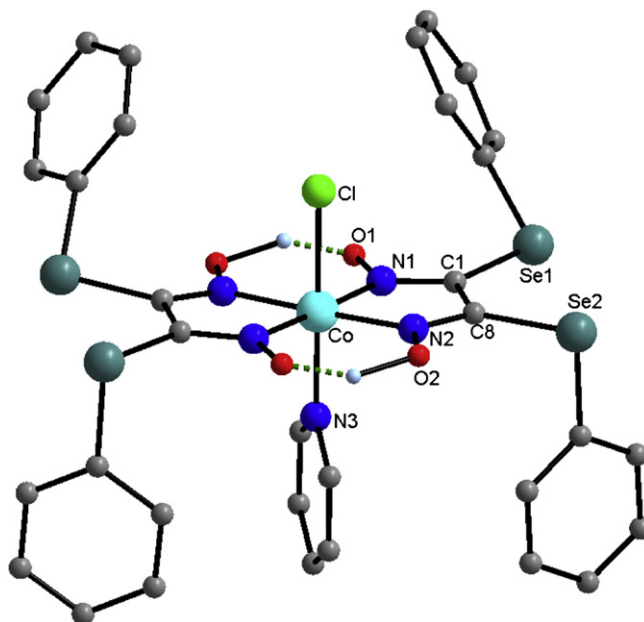
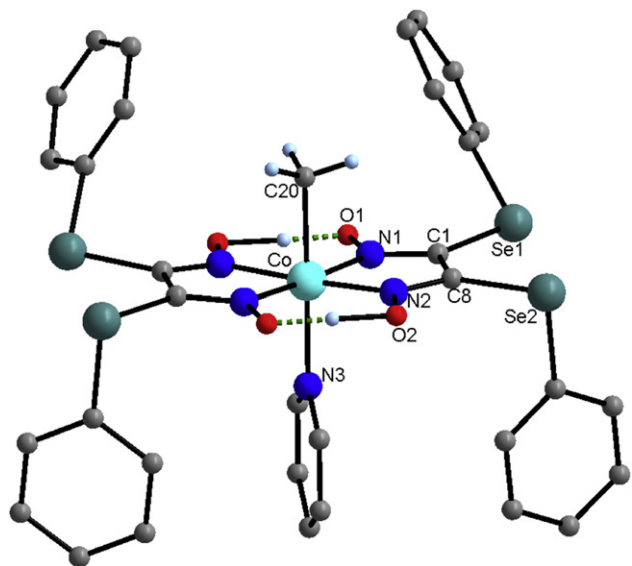
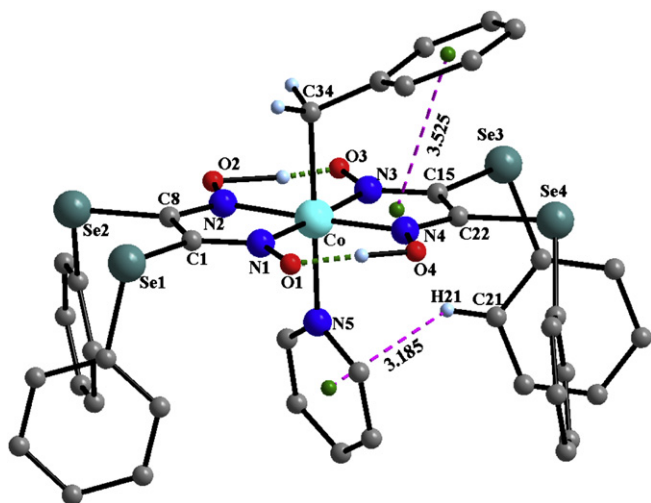
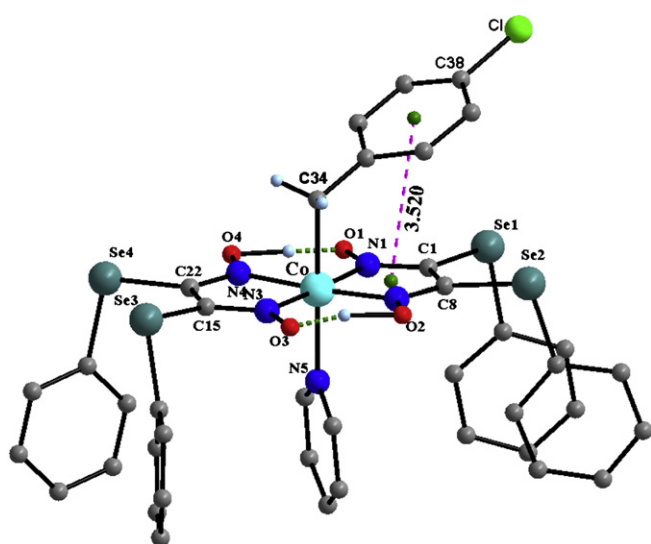


Fig. 1. Molecular structure of **1**.

Fig. 2. Molecular structure of **2**.Fig. 3. Molecular structure of **6**.Fig. 4. Molecular structure of **7**.**Table 2**Selected bond lengths, bond angles and other relevant structural parameters for **1**, **2**, **6**, and **7**.

parameters	1	2	6	7
Co–C/X (Å)	2.224(2)	1.992(5)	2.077(5)	2.073(6)
Co–N _{py} (Å)	1.971(6)	2.064(5)	2.070(4)	2.061(5)
X/C–Co–N _{py} (°)	177.9(2)	175.7(3)	174.7(2)	175.1(3)
α (°)	+3.98(28)	+6.84(19)	−0.78(15)	+1.96(14)
τ (°)	90.0	90.0	68.2(4)	89.9(7)
<i>d</i> (Å)	+0.0314(11)	+0.0530(8)	+0.0431(7)	+0.0479(9)
$\pi \cdots \pi$ (Å)			3.525(1)	3.5204(9)

bond length increases from 1.992(5) Å in **2** to 2.077(5) Å in **6** with increasing bulk of alkyl group.

Due to flexibility, the Co(dSePhgH)₂ unit undergoes geometrical deformation which is roughly represented by the displacement of cobalt atom from mean equatorial N4 plane (*d*) [33] and by the butterfly bending angle between two dioxime units (α) [33]. The deviations of the central cobalt atom from equatorial N4 plane are +0.0314(11), +0.0530(8), +0.0431(7) and +0.0479(9) Å in **1**, **2**, **6** and **7** respectively. The deviation is small and is toward the axial pyridine in all cases. The butterfly bending angle in **2** is +6.84° and is much larger than the reported value in MeCo(dioxime)₂Py complexes (dpgH, 4.7°; dmgH, 3.2°; gH, 2.0°), but slightly smaller than MeCo(dmestgH)₂Py complex [22]. The corresponding values in **1**, **6** and **7** are +3.98, −0.78 and +1.96°, respectively.

The pyridine ring is practically planar in all cases and is parallel to the dioxime C–C bond bonds in **1**, **2** and **7**. Its conformation being defined by the twist angles (torsion angle, τ)² 90.0, 90.0 and 89.9° in **1**, **2**, and **7**. The complex **6** has very low twist angle (68.2°) and the plane of pyridine lies below one of the N–O bonds of the dioxime. Also, pyridine is inclined toward one dioxime wing (C31–N5–Co) by 170.51°, which is unusual and unique for an organocobaloxime. This may have resulted from the strong C–H \cdots π interaction [C21–H21 \cdots π (Py) = 3.1849(7) Å, Fig. 3].

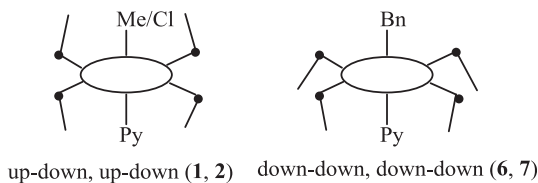
3.4. Orientation of SePh groups with respect to dioxime plane

In an extensive work on RCo(DBPh₂)₂L complexes with different R and L axial ligands by NMR and X-ray, Randaccio and coworkers have shown that the nature of the axial ligands determines the conformation of the equatorial moiety (phenyl groups of BPh₂) [34–37]. They suggested that the steric bulk of the axial ligand and its electronic interactions with the axial phenyls of the BPh₂ groups played an important role. Recently we showed that the SPh groups in RCo(dSPhgH)₂Py complexes adopted different conformations depending of the steric bulk of R and also, the structure and NMR were affected by the orientation of the SPh groups [24]. On the similar lines, SePh groups in **1**, **2**, **6** and **7** adopt different conformations in the solid state, for example, SePh groups exhibit up-down, up-down conformation in **1** and **2**, and down-down, down-down conformation in **6** and **7**. This occurs because the benzyl group is more bulky than Cl or Me and its free rotation along the Co–C bond leads to steric interactions with the equatorial SePh groups (Scheme 2).

3.5. Reactivity studies

The inherently weak Co–C bond in the organocobaloximes undergoes homolytic cleavage with visible light, similar to the

² The torsion angle (τ) is the angle between two virtual planes that bisect cobaloxime plane. This shows dihedral angle between the plane of pyridine and the plane bisecting the C–C bond of two dioxime units through the cobalt atom.



Scheme 2. Schematic representation of orientation of SePh groups with respect to dioxime plane in **1**, **2**, **6** and **7**.

activation of vitamin B₁₂ by apoenzyme [6,38–40] and the insertion of molecular oxygen into the Co–C bond has extensively been used to test the reactivity of these complexes [41–48]. Since the stability of the Co–C bond is affected by the dioxime (*cis*-influence) [23], we have studied the Co–C bond reactivity in complexes **6** and **7** by measuring the rate of oxygen insertion under photolytic conditions. The benzyl system has been particularly chosen since the Co–C bond is inherently weak and also the weak interaction between the benzyl group and the dioxime moiety might influence the Co–C bond reactivity [31,49]. The reaction obeys a pseudo-first-order rate law and the rates lie between the *dmestgH* and *dpgH* complexes (Table 3). The overall rate follows the order *dmestgH* > *dSPhgH* > *dpgH* > *dSPhgH* ≥ *dmgH* > *gH*. The variation of substituent in the dioxime from carbon to SPh does not change the rate much; however change with SePh has led to faster rate of oxygen insertion.

A significant reactivity difference in oxygen insertion in **6** and **7** has been observed, although the Co–C bond length is similar in both cases. Recently we have proposed that the puckering in the Co(dioxime)₂ (α and d values) influences the Co–C bond reactivity [32]. This may be the case here also; the d values are similar but α values are different and changes from negative to positive in complexes **6** and **7**, respectively. The puckering of dioxime plane towards the axial R group (positive α value) might be the reason for higher rate in **7** as compared to the complex **6**.

3.6. Description of the molecular structure of **8**

A slow evaporation of solvent from the solution of **8** (CH₂Cl₂/CH₃OH) resulted in the formation of brown crystals suitable for X-ray studies. Details about data collection, refinement, and structure solution are summarized in Table 1 and molecular structure with selected numbering schemes is shown in Fig. 5. Selected geometrical parameters are given in Table 4 and are compared with the known dioxy complexes containing Co(O₂) bound to a primary carbon atom. The SePh groups in **8** exhibit up-down, up-down conformation; similar to the confirmation in **1** and **2** and indicates that the steric interaction of the axial benzyl group with the equatorial SePh groups is decreased after the oxygen insertion.

A significant parameter for the peroxide compounds is the R–O–O–R' dihedral angle and it is governed by the bond pair-lone pair (BP–LP) and LP–BP interactions around the O–O bond. The

Table 3
Pseudo-first-order rate constant (k_{obs}) for oxygen insertion in RCo(dioxime)₂Py.

RCo(dioxime) ₂ Py	k_{obs} (s ⁻¹)	Ref.
BnCo(<i>gH</i>) ₂ Py	7.1×10^{-4}	[23]
BnCo(<i>dmgH</i>) ₂ Py	1.2×10^{-3}	[23]
BnCo(<i>dpgH</i>) ₂ Py	4.8×10^{-3}	[23]
BnCo(<i>dSPhgH</i>) ₂ Py	1.29×10^{-3}	[32]
BnCo(<i>dmestgH</i>) ₂ Py	5.0×10^{-2}	[23]
BnCo(<i>dSePhgH</i>) ₂ Py	6.95×10^{-3}	this work
4-ClBnCo(<i>dSePhgH</i>) ₂ Py	1.13×10^{-2}	this work

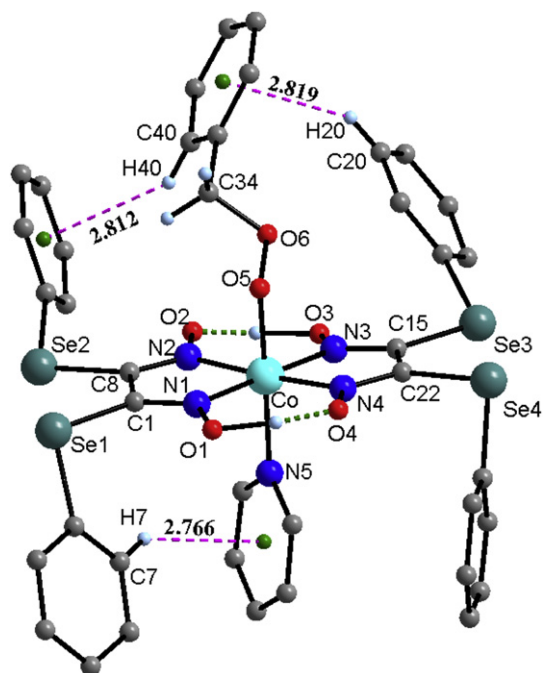


Fig. 5. Molecular structure of **8**.

complex **8** has the highest value of dihedral angle (124.5°) whereas it is lowest in complex **A** (106.2°). The higher the dihedral angle the greater the BP–LP interaction. The steric *cis* interaction of [Co(dioxime)₂] moiety with the axial ligand is much smaller in the present complex than the reported dioxy complexes as it contains the lowest Co–O–O bond angle (110° vs 116°).

The orientation of the benzyl group in **8** is guided by strong C–H... π interactions with the dioxime and this has led to O–O and C–C(Ph) plane almost parallel (178°) to each other. This has partially resulted from the π ... π interaction (3.666 Å) between the phenyl rings of benzyl groups in the crystal packing (Figure S3).

The data in Table 4 shows that the Co–O, Co–N_{py}, and O–O bond distances in **8** do not differ significantly from the reported oxygen-inserted complexes (**A**, **B**, and **C**), however, equatorial dioxime plane is somewhat puckered in the former as it contains high α value. The large α value may have resulted due to the C–H... π interactions and the crystal packing.

Table 4
Selected bond lengths, bond angles and structural parameters for **8** and comparison with other dioxy complexes (**A** = 4–CNC₆H₄CH₂(O₂)Co(*dmestgH*)₂Py [23]; **B** = 2-naphthylCH₂(O₂)Co(*dmestgH*)₂Py [23]; **C** = Bn(O₂)Co[dS(3,5–Me₂C₆H₃)*gH*]₂Py [32]).

parameters	8	A	B	C
Co–O _{ax} (Å)	1.866(3)	1.896(2)	1.875(4)	1.891(5)
Co–N _{py} (Å)	2.004(4)	1.995(3)	1.978(4)	1.991(5)
O–O (Å)	1.466(4)	1.435(3)	1.399(5)	1.424(6)
O–C (Å)	1.411(7)	1.421(4)	1.446(7)	1.433(7)
Co–O–O (°)	110.9(3)	116.43(17)	116.5(3)	116.0(3)
O–O–C (°)	106.0(4)	107.5(2)	108.1(4)	103.8(4)
Co–O–O–C (°)	124.5(4)	106.2(2)	–114.0(4)	–114.4(5)
O–C–C (°)	106.3(4)	115.4(3)	105.3(5)	108.4(5)
O–O–C–C (°)	178.1(4)	60.8(4)	175.3(5)	–165.6(5)
N _{py} –Co–O _{ax} (°)	174.21(17)	173.80(11)	171.8(2)	173.5(3)
d (Å)	+0.0190(8)	+0.011	+0.021	+0.007(9)
α (°)	+6.09(17)	3.24(11)	3.37(21)	+1.105(15)
τ (°)	66.92(16)	79.84(8)	88.60(10)	68.77(14)
C–H... π (Å)		3.079(1)	3.110(2)	

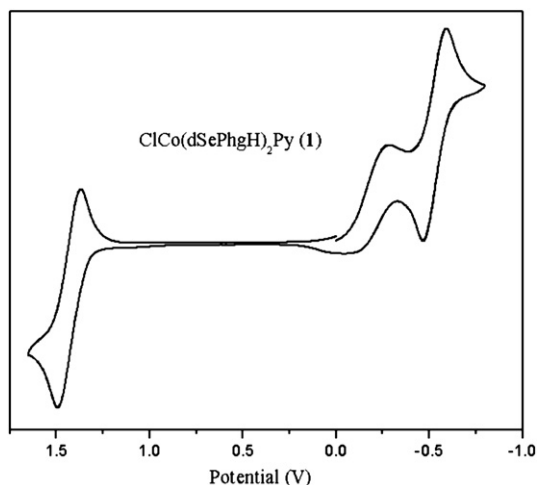


Fig. 6. Cyclic voltammogram of **1** in CH_2Cl_2 with 0.1 M $n\text{Bu}_4\text{NPF}_6$ as supporting electrolyte at 0.1 V/s at 25 °C.

3.7. Electrochemical studies (cyclic voltammetry)

The electrochemical behavior of **1–3** has been studied to understand the effect of dioxime (dSePhgH) on the redox potentials of the cobalt center. The cyclic voltammograms are shown in Figs. 6 and 7, and the CV data are given in Table 5. The cyclic voltammogram of **1** (Fig. 6) shows one irreversible peak at -0.285 V and one quasi-reversible peak ($E_{1/2} = -0.530$ V) in the reductive half corresponding to Co(III)/Co(II) and Co(II)/Co(I), respectively. In the oxidation half only one quasi-reversible wave corresponding to Co(IV)/Co(III) ($E_{1/2} = 1.430$ V) is observed. A similar cyclic voltammogram was shown by $\text{ClCo}(\text{dSPhgH})_2\text{Py}$ [24]. However, on comparison of these values with those for $\text{ClCo}(\text{dSPhgH})_2\text{Py}$, complex **1** is more difficult to reduce from Co(III)/Co(II) and from Co(II)/Co(I) (Table S6).

The cyclic voltammograms of the organocobaloximes (**2** and **3**) show only one irreversible reduction response corresponding to Co(III)/Co(II) at -1.155 and -1.174 V, respectively (Fig. 7). In the oxidative half a quasi-reversible one-electron oxidation wave corresponding to Co(IV)/Co(III) is observed. The $E_{1/2}$ value for this process is 1.223 and 1.178 V in complex **2** and **3**, respectively. Due to the higher electron donation ability of the alkyl groups, the Co(III)/Co(II) redox process in **2** and **3** is considerably cathodically

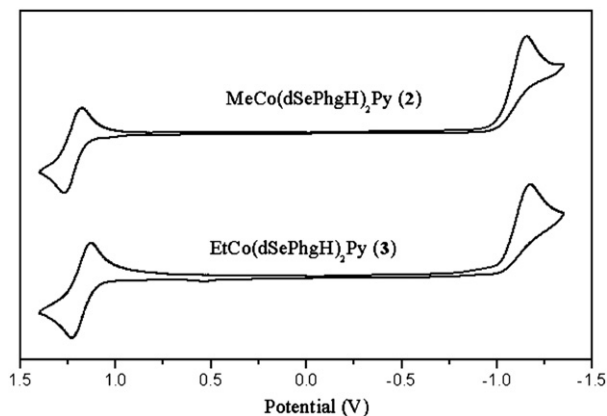


Fig. 7. Cyclic voltammograms of **2** and **3** in CH_2Cl_2 with 0.1 M $n\text{Bu}_4\text{NPF}_6$ as supporting electrolyte at 0.1 V/s at 25 °C.

Table 5

CV Data for **1–3** in CH_2Cl_2 and $n\text{Bu}_4\text{NPF}_6$ at 0.1 V/s at 25 °C.

No	Co(III)/Co(II)		Co(II)/Co(I)		Co(IV)/Co(III)	
	E_{pc}^a (V)	E_{pc}^b (V)	$E_{1/2}(\text{V})^a$ (ΔE_p (mV))	$E_{1/2}^b$ (V)	$E_{1/2}(\text{V})^a$ (ΔE_p (mV))	$E_{1/2}^b$ (V)
1	-0.285	-0.711	-0.530(125)	-0.957	1.430 (124)	1.003
2	-1.155	-1.582	–	–	1.223 (89)	0.796
3	-1.174	-1.601	–	–	1.178 (99)	0.751

^a Vs. Ag/AgCl.

^b Vs. Fc/Fc⁺ ($E_{1/2} = 0.4269$ V).

shifted and hence the Co(II)/Co(I) response is further cathodically shifted and is not observed even down to -1.5 V. The values show that the electrochemical reduction of **2** and **3** is easier as compared to the alkyl cobaloxime with the dSPhgH equatorial ligand (Table S6).

4. Conclusion

The synthesis and characterization of a new series of cobaloximes with bis(phenylselanyl)glyoxime as equatorial ligand has been described. The reactivity of benzyl cobaloximes with molecular oxygen has been examined and the rate of insertion depends on the dioxime and follow the order $\text{dmestgH} > \text{dSePhgH} > \text{dpgH} > \text{dSPhgH} \geq \text{dmgH} > \text{gH}$. The conformation of the SePh groups in the benzyl cobaloxime and its dioxy product is different and indicates that the steric interaction of the axial benzyl group with the equatorial SePh groups is decreased after the oxygen-insertion.

Acknowledgement

This work has been supported by the grants from DST and CSIR, India. K. K. thanks UGC, New Delhi, India for Senior Research Fellowship.

Appendix A. Supplementary material

CCDC 819076–819080 contains the supplementary crystallographic data for this paper. These data can be obtained free of charge from The Cambridge Crystallographic Data Centre via www.ccdc.cam.ac.uk/data_request/cif.

Appendix. Supplementary material

Supplementary data associated with this article can be found, in the online version, at [doi:10.1016/j.jorganchem.2011.07.012](https://doi.org/10.1016/j.jorganchem.2011.07.012).

References

- [1] L. Randaccio, N. Bresciani-Pahor, E. Zangrando, L.G. Marzilli, *Chem. Soc. Rev.* 18 (1989) 225–250.
- [2] N. Bresciani-Pahor, M. Forcolin, L.G. Marzilli, L. Randaccio, M.F. Summers, P.J. Toscano, *Coord. Chem. Rev.* 63 (1985) 1–125 (and refs cited therein).
- [3] L. Randaccio, *Comments Inorg. Chem.* 21 (1999) 327–376.
- [4] D. Dolphin (Ed.), *B12*, Wiley & Sons, New York, 1982.
- [5] R. Banerjee, *Chemistry and Biochemistry of B12*, Wiley & Sons, Inc, N. Y., 1999.
- [6] K.L. Brown, *Chem. Rev.* 105 (2005) 2075–2149.
- [7] L.G. Marzilli, M.F. Summers, N. Bresciani-Pahor, E. Zangrando, J.-P. Charland, L. Randaccio, *J. Am. Chem. Soc.* 107 (1985) 6880–6888.
- [8] M.F. Summers, L.G. Marzilli, N. Bresciani-Pahor, L. Randaccio, *J. Am. Chem. Soc.* 106 (1984) 4478–4485.
- [9] C. Huilan, H. Deyan, L. Tian, Y. Hong, T. Wenxia, J. Chen, P. Zheng, C. Chen, *Inorg. Chem.* 35 (1996) 1502–1508 (and refs cited therein).
- [10] G. Costa, G. Mestroni, E.d. Savorgnani, *Inorg. Chim. Acta* 3 (1969) 323–328.
- [11] G. Costa, *Pure Appl. Chem* 30 (1972) 335–352.
- [12] B.D. Gupta, R. Yamuna, V. Singh, U. Tiwari, *Organometallics* 22 (2003) 226–232.
- [13] C. López, S. Alvarez, X. Solans, M. Font-Altaba, *Inorg. Chim. Acta* 121 (1986) 71–75.

- [14] P.J. Toscano, T.F. Swider, L.G. Marzilli, N. Bresciani-Pahor, L. Randaccio, *Inorg. Chem.* 22 (1983) 3416–3421.
- [15] N. Bresciani-Pahor, L. Randaccio, E. Zangrando, P.J. Toscano, *Inorg. Chim. Acta* 96 (1985) 193–198.
- [16] D. Dodd, M.D. Johnson, B.L. Lockman, *J. Am. Chem. Soc.* 99 (1977) 3664–3673.
- [17] B.D. Gupta, K. Qanungo, T. Barclay, W. Cordes, *J. Organomet. Chem.* 560 (1998) 155–161.
- [18] B.D. Gupta, K. Qanungo, R. Yamuna, A. Pandey, U. Tiwari, V. Vijaikanth, V. Singh, T. Barclay, W. Cordes, *J. Organomet. Chem.* 608 (2000) 106–114.
- [19] C. López, S. Alvarez, M. Font-Bardia, X. Solans, *J. Organomet. Chem.* 414 (1991) 245–259.
- [20] C. López, S. Alvarez, X. Solans, M. Font-Bardia, *Polyhedron* 11 (1992) 1637–1646.
- [21] P.J. Toscano, L. Lettko, E.J. Schermerhorn, J. Waechter, K. Shufon, S. Liu, E.V. Dikarev, J. Zubieta, *Polyhedron* 22 (2003) 2809–2820.
- [22] D. Mandal, B.D. Gupta, *Organometallics* 24 (2005) 1501–1510.
- [23] M. Bhuyan, M. Laskar, D. Mandal, B.D. Gupta, *Organometallics* 26 (2007) 3559–3567.
- [24] G. Dutta, K. Kumar, B.D. Gupta, *Organometallics* 28 (2009) 3485–3491.
- [25] *International Tables for X-ray Crystallography*; Kynoch Press: Birmingham, England, 1974; vol. IV.
- [26] *Smart & SAINT Software Reference manuals, Version 6.45*; Bruker Analytical X-ray Systems, Inc.: Madison, WI, 2003.
- [27] G.M. Sheldrick, *SADABS, Software for Empirical Absorption Correction, Ver. 2.05*. University of Göttingen, Göttingen, Germany, 2002.
- [28] *XPREP, 5.1 ed.*; Siemens Industrial Automation Inc.: Madison, WI, 1995.
- [29] G.M. Sheldrick, *SHELXL97, Program for Crystal Structure Refinement*. University of Göttingen, Göttingen, Germany, 2008.
- [30] $\Delta\delta(^{13}\text{C}_{\text{C}=\text{N}})$ value has been taken instead of $\delta(^{13}\text{C}_{\text{C}=\text{N}})$. This is to avoid the direct effect of substituent on $\delta(\text{C}=\text{N})$ value.
- [31] D. Mandal, B.D. Gupta, *Organometallics* 26 (2007) 658–670.
- [32] G. Dutta, B.D. Gupta, *J. Organomet. Chem.* 696 (2011) 892–896.
- [33] Positive sign of α and δ indicates bending towards R and displacement toward base and vice versa.
- [34] F. Asaro, R. Dreos, G. Nardin, G. Pellizer, S. Peressini, L. Randaccio, P. Siega, G. Tazher, C. Tavagnacco, *J. Organomet. Chem.* 601 (2000) 114–125.
- [35] R. Dreos, S. Geremia, G. Nardin, L. Randaccio, G. Tazher, S. Vuano, *Inorg. Chim. Acta* 272 (1998) 74–79.
- [36] R. Dreos, G. Tazher, S. Vuano, F. Asaro, G. Pellizer, G. Nardin, L. Randaccio, S. Geremia, *J. Organomet. Chem.* 505 (1995) 135–138.
- [37] F. Asaro, R. Dreos, S. Geremia, G. Nardin, G. Pellizer, L. Randaccio, G. Tazher, S. Vuano, *J. Organomet. Chem.* 548 (1997) 211–221.
- [38] K.L. Brown, *Dalton Trans.* (2006) 1123–1133.
- [39] J.M. Pratt, B.R.D. Whitera, *J. Chem. Soc. A* (1971) 252–255.
- [40] D.N.R. Rao, M.C.R. Symons, *J. Chem. Soc. Faraday Trans. 1* (1984) 423–434.
- [41] C. Fontaine, K.N.V. Duong, C. Marianne, A. Gaudemer, C. Giannotti, *J. Organomet. Chem.* 38 (1972) 167–178.
- [42] C. Marianne, C. Giannotti, A. Gaudemer, *J. Organomet. Chem.* 54 (1973) 281–290.
- [43] J. Deniau, A. Gaudemer, *J. Organomet. Chem.* 191 (1980) C1–C2.
- [44] M. Kijima, H. Yamashita, T. Sato, *J. Organomet. Chem.* 474 (1994) 177–182.
- [45] B.D. Gupta, S. Roy, *Inorg. Chim. Acta* 108 (1985) 261–264.
- [46] B.D. Gupta, M. Roy, I. Das, *J. Organomet. Chem.* 397 (1990) 219–230.
- [47] B.D. Gupta, V. Vijaikanth, V. Singh, *J. Organomet. Chem.* 570 (1998) 1–7.
- [48] G. Dutta, M. Laskar, B.D. Gupta, *Organometallics* 27 (2008) 3338–3345.
- [49] D. Mandal, B.D. Gupta, *Organometallics* 25 (2006) 3305–3307.